On the Reconstruction of NQR Nutation Spectra in Solids with Powder Geometry

H. Robert and D. Pusiol

Facultad de Matemática, Astronomía y Física, Universidad Nacional de Córdoba,
Ciudad Universitaria, 5000 Córdoba, Argentina

E. Rommel and R. Kimmich

Sektion Kernresonanzspektroskopie, Universität Ulm, 89069 Ulm, Germany

Z. Naturforsch. **49a**, 35–41 (1994); received August 14, 1993

In single crystals the NQR nutation frequency depends on the relative orientation of the coil and the quadrupole axes. In powders the nutation lineshape is a superposition of spectra from the randomly oriented single crystals, so that powder patterns appear in such experiments if the reconstruction is performed by the Fourier transform method. In this paper an alternative reconstruction method of nutation spectra is suggested making use of the Hankel Transform. In this way the nutation spectra are simplified. Singularities arising with experiments for the determination of the asymmetry parameter η can easily be resolved. In the particular case of an axially symmetric quadrupolar tensor and a homogeneous radiofrequency field one can reduce the powder pattern to a single line without heterogeneous broadening with respect to orientation. Further improvement of the nutation spectra can be achieved by taking advantage of the maximum entropy method, which strongly reduces apodisation and noise problems. Applications of the new data manipulation techniques to NQR imaging methods published elsewhere and 2D zero-field NQR spectroscopy are reported.

1. Introduction

Two-dimensional techniques in nuclear quadrupole resonance spectroscopy (2D-NQRS) have recently been developed for several applications in powder materials. Zero-magnetic-field nutation spectroscopy has been used to measure the asymmetry parameter, η, [1, 2], and spatially resolved NQR spectra (ϱNQR Imaging) [3, 4]. In these two-dimensional experiments the variable radio frequency (RF) pulse is used to encode information in one frequency dimension (leading to nutation spectra) and a second frequency domain referring to free evolution of the magnetization after the resonant RF pulse (providing pure NQR spectra). Both variants of this technique are amplitude modulated rotating frame experiments. The two-dimensional time-domain signal $S(t, t_p)$ is detected during the free-evolution time t for varying pulse widths t_p. Instead of the pulsewidths, the RF amplitude can be varied equivalently. One thus distinguishes the proper free-induction decay (FID), $S = S(t, t_p = \text{const})$, from the pseudo-FID, $S = S(t = \text{const},\ t_p)$, where "const" refers to certain fixed values. The problem we are addressing now is to find suitable procedures to transform the two-dimensional time-domain signal into a two-dimensional spectrum.

In an NQR experiment the RF coil defines a preferential axis. Both the nutation frequency,

$$\omega_1 = \frac{1}{2\sqrt{3}\,\xi}\,\gamma B_1\,, \tag{1}$$

where B_1 is the amplitude of the RF flux density, γ the gyromagnetic ratio and $\xi = \left(1 + \frac{\eta^2}{3}\right)^{1/2}$, and the amplitudes of the FID after the pulse depend on the relative orientation of the principal axes of the electric field gradient (EFG) tensor and the coil axis. With powdery materials the pseudo-FID consists of a superposition of contributions for all relative orientations between the EFG principal axes and the coil axis. Fourier processing of the pseudo-FID therefore leads to a powder pattern in the ω_1 dimension [1, 2] rather than the pure, unsuperimposed lines. This may lead to severe inconveniences in the interpretation of the spectra.

---

* Presented at the XIIth International Symposium on Nuclear Quadrupole Resonance, Zürich, July 19–23, 1993.

Reprint requests to Dr. H. Robert and Dr. D. Pusiol, Facultad de Matemática, Astronomia y Fisica, Universidad Nacional de Córdoba, Ciudad Universitaria, 5000 Córdoba, Argentina.

In this paper we suggest to evaluate the pseudo-FID by the aid of the Hankel transform instead of the conventional Fourier transform (FT). The nutation spectra used for instance for the determination of η can then be evaluated more easily because the singularities of the spectrum reveal themselves in a very distinct way. With NQR imaging experiments with powdery materials, on the other hand, an elegant and reliable image reconstruction procedure is given.

The second objective of this work is to introduce the so-called maximum entropy method (MEM) [5–7] to 2D NQR spectroscopy leading to considerable improvements of the data processing. Problems due to weak signal-to-noise ratios and to inefficient apodisation can be circumvented in this way.

2. Theoretical Background

The response function $S(t,t_p)$ of spins 3/2 in axially symmetric electric field gradients to transient RF irradiation has first been derived by Bloom et al. [8]. This theory was later extended for the axially asymmetric case by Pratt et al. [9]. According to this formalism, the two-dimensional time-domain signal $S(t,t_p)$ can be factorized into independent response functions, $Q(t)$ and $R(t_p)$, for the two time domains:

$$S(t,t_p) \sim Q(t)\, R(t_p)\,. \tag{2}$$

$Q(t)$ is the inverse Fourier transform of the pure NQR spectrum, $Q(t)=\mathscr{F}^{-1}\{G(\omega)\}$. $R(t_p)$ is generally given by

$$R(t_p) \sim \int_0^\infty \mathrm{d}z\,\varrho(z) B_1(z) \int_0^\pi \mathrm{d}\theta \int_0^{2\pi} \mathrm{d}\phi\, \sin\theta\, F(\theta,\phi) \cdot \sin[F(\theta,\phi)\,\omega_1(z)\, t_p]\,, \tag{3}$$

where the case of inhomogeneous $B_1 = B_1(z)$ fields is included. $\varrho(z)$ is the local spin density. The function $F(\theta,\phi)$ is defined by

$$F(\theta,\phi) = [4\eta^2 \cos^2(\theta) + \sin^2(\theta)\,(9+\eta^2+6\eta\cos(2\phi))]^{1/2}\,, \tag{4}$$

where θ and ϕ are the polar and azimuthal angles, respectively, of the largest EFG tensor principal axis with respect to the coil axis. The relaxation decay during t_p is neglected for simplicity.

Carrying out the Fourier transform with respect to t provides the spectrum:

$$\tilde{S}(\omega,t_p) \sim G(\omega)\, R(t_p)\,. \tag{5}$$

$G(\omega)$ represents the full NQR spectroscopic information. The pseudo-FID $\tilde{S}(\omega_i,t_p)$ is obtained by keeping the resonance frequency at a fixed value ω_i of the NQR spectrum. The nutation spectrum is obtained by deconvoluting the pseudo-FID $\tilde{S}(\omega_i,t_p)$ as shown in the following section.

For the special case $\eta=0$, the pseudo-FID is given by

$$\tilde{S}(\omega_i,t_p) \sim G(\omega_i) \int_0^\infty \mathrm{d}z\,\varrho(z)\, B_1(z) \int_0^\pi \mathrm{d}\theta \cdot \sin^2\theta\, \sin[\omega_1(z)\, t_p \sin\theta]\,. \tag{6}$$

The inner integral can be represented by a series of Bessel functions of the first kind, J_n [8]. We have then

$$\tilde{S}(\omega_i,t_p) \sim G(\omega_i) \int_0^\infty \mathrm{d}z\,\varrho(z)\, B_1(z) \left[\frac{8}{3} J_1(\omega_1(z)\, t_p) - \sum_{n=1}^{\infty} \frac{J_{2n+1}(\omega_1(z)\, t_p)}{(2n+1)(2n-1)(2n+3)}\right]. \tag{7}$$

Taking into account the orthogonality property of Bessel functions, the solution of this integral equation can be expressed by the Hankel transform (HT) defined by the operation for a function $f(\omega_1 t_p)$

$$\tilde{f}(\omega) = \mathscr{H}_1\{f(\omega_1 t_p)\} = \int_0^\infty \mathrm{d}t_p\, t_p\, J_1(\omega t_p)\, f(\omega_1 t_p)\,. \tag{8}$$

The local spin density is then given by

$$\varrho(z) \sim \frac{\omega_1(z)}{B_1(z)} \left|\frac{\mathrm{d}\omega_1(z)}{\mathrm{d}z}\right| \int_0^\infty \mathrm{d}t_p\, t_p\, J_1(\omega_1(z) t_p)\, \tilde{S} f(\omega_1 t_p)\,, \tag{9}$$

where we have made use of the delta function relation [10]

$$\delta(g(x)) = \frac{\delta(x-x_0)}{\left|\dfrac{\mathrm{d}g}{\mathrm{d}x}\right|}\,, \tag{10}$$

where $g(x_0)=0$.

2.1 Measurement of the Tensor-Asymmetry Parameter

With the 2D zero-field NQR experiment proposed by Harbison et al. [1], a homogeneous RF field is applied, so that the first integral in (7) refers to the first term only and can be replaced by a constant. Equation (7) leads to a nutation spectrum consisting of a single line by Hankel transforming the pseudo-FID, $\tilde{S}(\omega_i,t_p)$ rather than to a powder pattern produced by the Fourier transform suggested in [1] (compare Figure 1). In the case of asymmetric field-gradient tensors, the Hankel transform leads to modified powder pat-

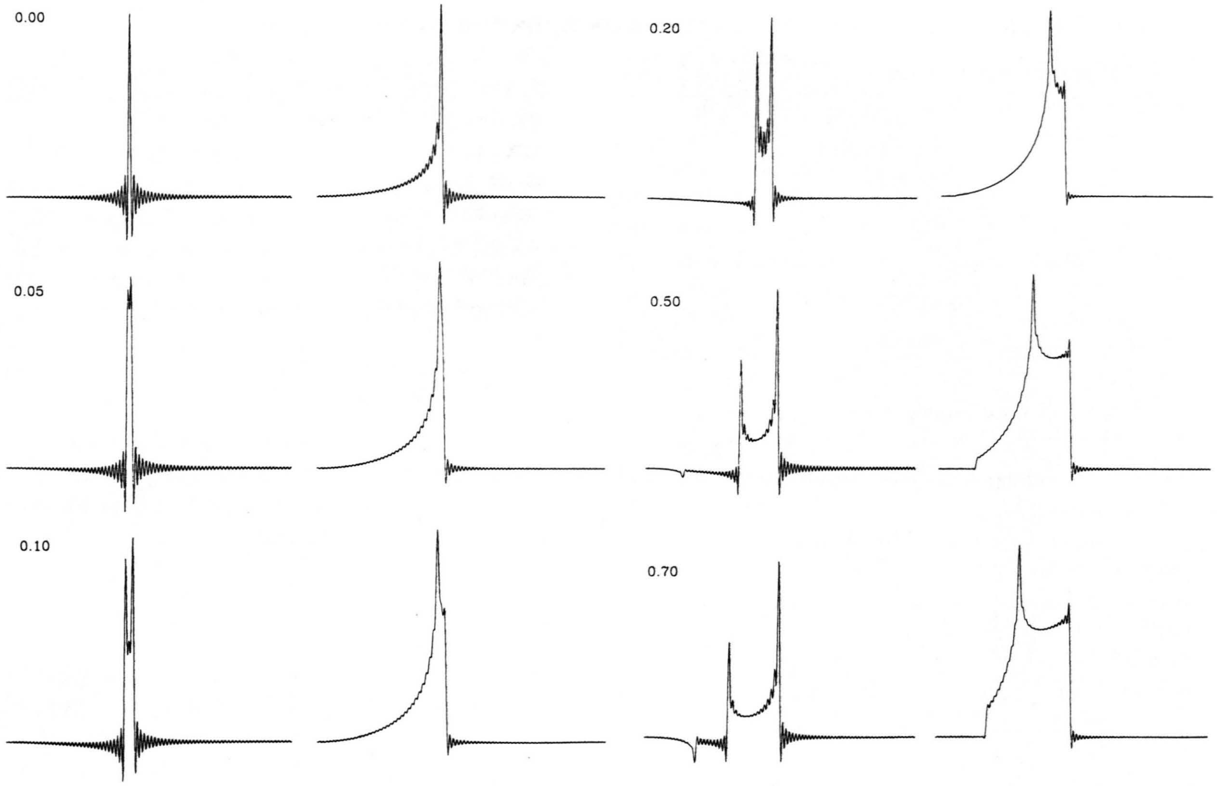

Fig. 1. Calculated nutation line-shapes (in the ω_1 dimension) for different values of the asymmetry parameter η. The reconstruction procedures were the Hankel (left) and Fourier (right) transforms. The numerical calculations of $\tilde{S}(\omega, t_p)$, were obtained by 160 θ data points in a range $0-\pi$, and 360 values of ϕ in the range $0-2\pi$. 512 data points were used for the Fourier as well as for the Hankel transformations.

terns which are narrower than those produced by the Fourier transform procedure. This was demonstrated by comparative computer simulations for different η values. The results are displayed in Figure 1. The wiggles and oscillations in the spectra obtained by Fourier as well as by Hankel transforms are due to the discrete increment of the variables in the numerical integration and to truncation of the pseudo-FID to a finite t_p interval.

The powder patterns calculated by the Hankel transform for $\eta \neq 0$ reveals the singularities ν_2 and ν_3 predicted by the analytical theory of Harbison. The positions of these singularities are just the same as expected with Fourier spectra. However, as demonstrated in Fig. 1, the Fourier method does not lead to a clear resolution even in the numerical simulation. For the experimental determination of η values on this basis, the Hankel procedure is therefore expected to be preferable in any case. The evaluation formula is according to Harbison et al. [1]

$$\eta = \frac{3(\nu_3 - \nu_2)}{\nu_3 + \nu_2}. \tag{11}$$

2.2 *ϱ NQR Imaging*

With the ϱNQR imaging technique for powdery solids [3, 4, 11], RF amplitudes depending linearly on the spatial coordinate z are applied, so that the position of the nuclei is encoded in the FID amplitudes. For the reconstruction of the spatially dependent density of nuclei, the Hankel transform can be used again for $\eta = 0$. The corresponding Hankel transform expression of (7) [12] is given in (9). This is an exact solution of the problem, in contrast to the direct Fourier transform evaluation suggested in our first paper on this subject [3]. Note, however, that the Fourier deconvolution method [13] also provides exact solutions and generally applies to any η value.

2.3 Data Evaluation by the Maximum Entropy Method

With the evaluation procedures described so far, the problem of wiggle artifacts due to finite pseudo-FID acquisition times and superimposed noise may severely restrict the applicability of the techniques. Even if extended t_p times could be probed from the experimental point of view, still the problem of temperature fluctuations of the sample in such long scan times can arise, so that shifts of the resonances occur.

As a much more favorable evaluation procedure we therefore suggest the maximum entropy method (MEM). This is a kind of deconvolution procedure, widely used in astronomy [5, 14], optical deconvolution [15, 16], medical tomography [17, 18], nuclear magnetic resonance (NMR) spectroscopy [6], and NMR imaging [7].

Basically, the idea of the MEM procedure for NQR purposes is to find a set of nutation lineshapes or profiles in imaging which are consistent with the experimental pseudo-FID. The criterion for the selection of a lineshape (or profile) out of this set is the minimum of the information content, or equivalently the maximum of the entropy. The detailed description of the method has been reported in [5–7]. In the following merely the principles are summarized.

The nutation spectrum reconstructed by fitting the experimental pseudo-FID is considered as a set of positive number $\{X_j\}$, $j=1, 2, \ldots, N$, which are to be determined. The discrete pseudo-FID data set, $\{\tilde{S}_p\}$, representing the response function, $\tilde{S}(\omega_i, t_p)$, can be expressed as

$$\tilde{S}_p = \sum_{j=1}^{N} D_{p,j} X_j \pm \sigma_p; \quad p=1, 2, \ldots, M, \tag{12}$$

where σ_p is the standard deviation of the noise; M and N are the numbers of points in the pseudo-FID and in the resulting nutation spectrum, respectively (in general we choose $N > M$) and $\mathbf{D}$ is the transfer matrix of the system, given by

$$D_{p,j} = \int_0^{\pi} \mathrm{d}\theta \int_0^{2\pi} \mathrm{d}\phi \sin\theta \, F(\theta,\phi) \sin[F(\theta,\phi)\omega_{1,j} t_p]. \tag{13}$$

Formally, the constraint on $\{X_j\}$ is introduced by comparing the actual data $\tilde{S}_p$ with the simulated data according to

$$\Gamma_p = \sum_{j=1}^{N} D_{p,j} X_j. \tag{14}$$

The misfit between the actual data set $\{\tilde{S}_p\}$ and the simulated set $\{\Gamma_p\}$ is characterized by the least-squares criterion of statistics

$$\chi^2 = \sum_{p=1}^{M} \frac{(\Gamma_p - \tilde{S}_p)^2}{\sigma_p^2}. \tag{15}$$

A reconstructed set $\{X_j\}$ is said to be feasible for selection using the maximum entropy criterion if the simulated data agree with the actual data set $\{\tilde{S}_p\}$ within the fluctuation range of noise, i.e. $\chi^2 \le M$. Restricting the $\{X_j\}$ to real and positive numbers, one can write the entropy $\mathcal{S}$ expression as

$$\mathcal{S} = -\sum_{j=1}^{N} \left(\frac{X_j}{A}\right) \ln\left(\frac{X_j}{A}\right), \tag{16}$$

where A is a background parameter, chosen as suggested in [7]. Here we use the Skilling/Bryan numerical algorithm [19] to select the feasible lineshape (or profile) which maximizes the entropy.

3. Experimental

The η measurements were carried out using a fully automated home made NQR spectrometer equipped with a PTS Mod 310 Synthesizer, a Doty Mod LN-2M preamplifier, a Motorola Mod AN779L power driver, a Motorola AN758 300 W transmitter and a Thurlby Mod 524 data acquisition system. The data were processed by a personal AT486 computer. The pulse programmer, quadrature detector, probehead, and software were home made. In order to avoid any drift of the sample temperature by RF power absorption, we used a two pulse sequence with a fixed duty cycle. The first pulse was the proper excitation pulse, the second was used as a dummy pulse. The length of the first pulse is t_p, that of the second $t_{p\,\max} - t_p$, where $t_{p\,\max}$ is the maximal pulse length in the experiment. The NQR signals were recorded in the interval between the two pulses.

An RF coil with 20 double windings was employed. The length was 30 mm the inner diameter 15 mm. The samples were purchased from Fluka and sealed in polytetrafluoropolyethylene (teflon) containers without further treatment such as recrystallization. The ϱNQR imaging experiment was performed following the procedure previously reported [20].

4. Results

Figures 2a and b show the nutation spectra of *p*-dichlorobenzene at room temperature, reconstructed

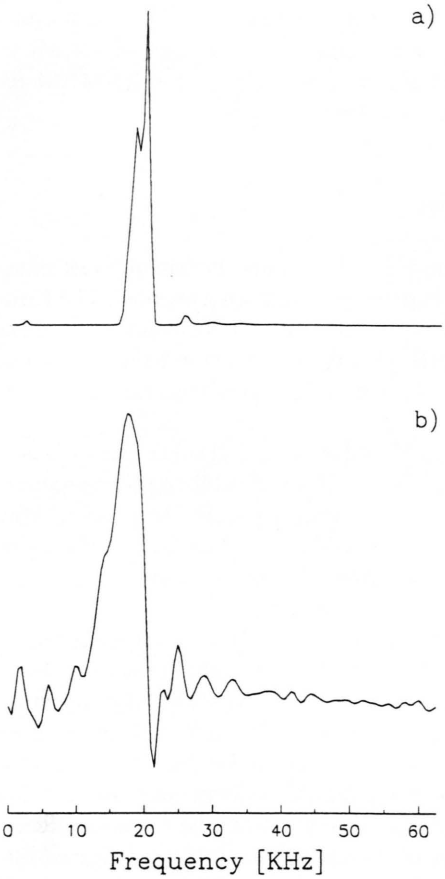

Fig. 2. a) Nutation spectrum, reconstructed by means of the MEM procedure. The background parameter was taken to be $A=10^{-3}$. The value of σ_p was 10% of the maximum value of the pseudo-FID. b) Fourier reconstructed nutation lineshape. The pseudo-FID was zero filled until 256 data points.

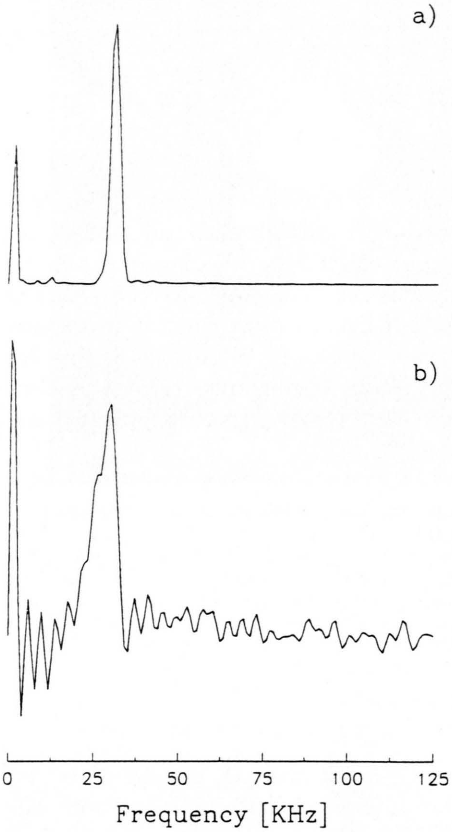

Fig. 3. Nutation spectra of TSC reconstructed by: a) MEM and b) Fourier transformation. A narrow line practically free of noise was obtained by means of the first procedure.

by means of MEM and the simple Fourier transform procedure, respectively. 128 data points were recorded per pseudo-FID. The increment of pulse width was $\Delta t_p = 4\,\mu s$. 10 FID's were accumulated in each case. The Fourier transform of the FID's was carried out using 1024 data points. The best experimental condition was found with a recycle delay of 1 s. The delay between the two pulses of a sequence was 4 ms.

The spectrum obtained with the MEM method (Fig. 2a) obviously has a much better quality than the pseudo-FID FFT spectrum (Fig. 2b). From the singularities, which are clearly resolved in the MEM spectrum, we obtain $\eta = 0.12$ in agreement with the literature value of 0.08 ± 0.03 [21]. The conventional Fourier reconstruction (Fig. 2b), on the other hand, does not reveal distinct singularities so that the asymmetry parameter cannot be determined on this basis.

A similar experiment was carried out in toluene-4-sulphonyl chloride (TSC). Figures 3 a and 3 b show the MEM and Fourier reconstructions of the nutation spectra, respectively. Distinct singularities could not be resolved so that a correspondingly small value of η must be concluded.

Figure 4 shows a two-dimensional ϱ NQR image of a test object of arsenic oxide. The picture was reconstructed (with respect to the nutation profile) using MEM, assuming an asymmetry parameter of $\eta = 0$. The test object was made of a plastic cylinder with two bores having cross sections with circular (diameter: 3.5 mm) and triangular (side length: 4.5 mm) shapes.

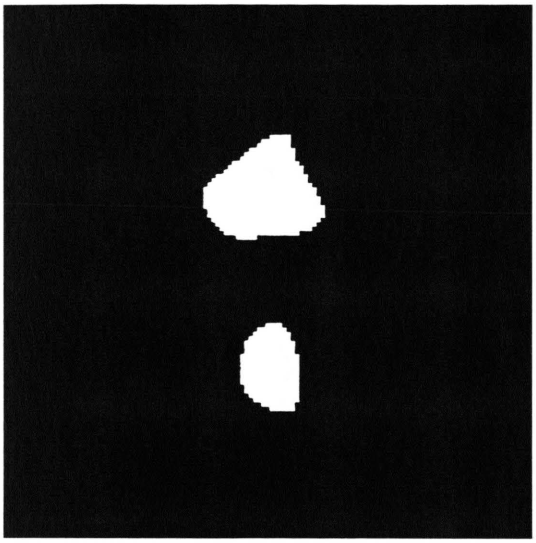

Fig. 4. Two-dimensional ϱ NQR image of a two-compartment sample filled with As_2O_3. The cross sections of the cylindric bores was circular and triangular, respectively. 50 projections on different directions of the RF gradient with respect to the sample were recorded and evaluated by the MEM procedure. The image finally was reconstructed by filtered back projection.

The bores were filled with As_2O_3 powder. Fifty projections of the sample with different orientations with respect to the RF coil axis were recorded. Each of them corresponds to one pseudo-FID. The set of pseudo-FID's was processed by the MEM procedure. The two-dimensional image was then reconstructed using filtered back projection [13]. The geometry of the test object obviously is well reproduced, whereas the deconvolution procedure applied in [13] lead to some artificial distortions of the image.

The MEM program was implemented in turbo Pascal language for running in an AT486 – 33 MHz clock – personal computer. The reconstructions by MEM of 128 points spectra shown in Figures 2a and 3a takes about 30 seconds. Instead, the FFT procedure was realized in several ten of milliseconds. The total acquisition time for the bidimensional images shown in Figure 4 was about 45 min. The total 2D-MEM reconstruction took about 40 min.

5. Conclusions

New methods for the reconstruction of NQR nutation spectra in general have been presented. The Hankel transform method exactly deconvolutes zero-field nutation spectra of spin 3/2 nuclei in axially symmetric EFG environments. The reconstruction of the nutation spectra of resonant nuclei in axially asymmetric field gradients by means of the Hankel method leads to simple nutation spectra with well-resolved singularities, so that the asymmetry parameter η can reliably be determined. In particular, the resolution of the singularities is superior to that of the conventional Fourier transform procedure.

The maximum entropy method as an replacement of the Hankel (or the Fourier) transform formalisms provides a particularly direct access to NQR nutation spectra or spatial profiles. It needs, however, more memory and computer processing time than the simple Fourier or Hankel Transform analysis. On the other hand, by means of MEM, the theoretically expected deconvolution function of the investigated system can be taken into account. Thus truncation and noise artifacts can virtually be avoided.

Acknowledgements

We thank the Alexander von Humboldt Foundation (Germany), Deutsche Forschungsgemeinschaft (DFG) (Germany), National Research Council of Argentina (CONICET), the Córdoba Provincial Research Council (Argentina), and Fundación Antorchas (Argentina) for financial support. One of us, H. R., acknowledges the Research Fellowship provided by CONICET. D. P. is a fellow of the CONICET.

[1] G. S. Harbison, A. Slokenbergs, and T. M. Barbara, J. Chem. Phys. **90,** 5292 (1989).
[2] G. S. Harbison and A. Slokenbergs, Z. Naturforsch. **45a,** 575 (1990).
[3] E. Rommel, P. Nickel, R. Kimmich, and D. Pusiol, J. Mag. Res. **91,** 630 (1990).
[4] E. Rommel, D. Pusiol, P. Nickel, and R. Kimmich, Meas. Sci. Technol. **2,** 866 (1991).
[5] S. F. Gull, and G. J. Daniell, Nature London **272,** 686 (1978).
[6] E. D. Laue, J. Skilling, J. Staunton, S. Sibisi, and R. Brereton, J. Magn. Reson. **62,** 437 (1985).
[7] G. J. Daniell and P. J. Hore, J. Magn. Reson. **84,** 515 (1989).
[8] M. Bloom, E. L. Hahn, and B. Hertzog, Phys. Rev. **97,** 1699 (1955).
[9] J. C. Pratt, P. Raganuthan, and C. A. McDowell, J. Magn. Reson, **20,** 313 (1975).
[10] J. D. Jackson, "Classical Electrodynamics", John Wiley & Sons, New York 1977.
[11] R. Kimmich, E. Rommel, Peter Nickel, and D. Pusiol, Z. Naturforsch. **47a,** 361 (1992).
[12] H. Robert, D. Pusiol, E. Rommel, and R. Kimmich, submitted for publication.
[13] E. Rommel, R. Kimmich, H. Robert, and D. Pusiol, Meas. Sci. Technol. **3,** 446 (1992).
[14] P. F. Scott, Mont. Not. Roy. Astron. Soc. **194,** 23p (1981).
[15] R. K. Bryan, and J. Skilling, Mont. Not. R. Astr. Soc. **191,** 69 (1980).
[16] B. R. Frieder and D. C. Wells, J. Opt. Soc. Amer. **68,** 93 (1978).
[17] G. Minerbo, Comp. Graph. Im. Proc. **10,** 48 (1979).
[18] M. C. Kemp, International Symposium on Radionuclide Imaging, IAEA-SM-247, **128,** Heidelberg.
[19] J. Skilling and R. K. Bryan, Mont. Not. Roy. Astron. Soc. **211,** 111 (1984).
[20] P. Nickel, E. Rommel, R. Kimmich, and D. Pusiol, Chem. Phys. Letters, **183,** 183 (1991).
[21] T. P. Das and E. L. Hahn, Nuclear Quadrupole Resonance Spectroscopy, Solid State Physics, Suppl 1, New York 1958.